Projected quasiparticle calculations for the $N=82$ odd-proton isotones

L. Losano
Departamento de Física, Universidade Federal da Paraíba, Caixa Postal 5008, 58059 João Pessoa, Paraíba, Brazil

H. Dias
Instituto de Física, Universidade de São Paulo, Caixa Postal 20516, 01498 São Paulo, São Paulo, Brazil
(Received 14 February 1991)

The structure of low-lying states in odd-mass $N=82$ isotones ($135 \leq A \leq 145$) is investigated in terms of a number-projected one- and three-quasiparticles Tamm-Dancoff approximation. A surface-delta interaction is taken as the residual nucleon-nucleon interaction. Excitation energies, dipole and quadrupole moments, and $B(M1)$ and $B(E2)$ values are calculated and compared with the experimental data.

I. INTRODUCTION

Theoretical studies of the $Z>50$, $N=82$ isotones, in the mass region $135 \leq A \leq 151$, show that the properties of low-lying states of these nuclei can be described by pure proton-quasiparticle excitations [1–6]. In Refs. [1–3], light odd isotones ($53 \leq Z \leq 65$) are studied with the usual Bardeen-Cooper-Schrieffer (BCS) formalism within the one- and three-quasiparticle space. The structure of light even isotones ($54 \leq Z \leq 62$) is investigated in terms of zero and two quasiparticles in Ref. [4], and, including particle-number projection in the formalism, heavy even-isotones ($62 \leq Z \leq 68$) are explained in Ref. [5]. More recently, using a seniority truncation method, Andreozzi *et al.* [6] performed a calculation of pairing effects in even isotones, with seniority $\nu \leq 4$ states and, in odd isotones, with $\nu=1$ states.

In the present work we study odd-mass isotones ($55 \leq Z \leq 63$) by means of a standard Tamm-Dancoff approximation in a number-projected one- and three-quasiparticle space (PBCS). The projection is performed after the minimization of the ground-state energy. As a residual two-body force, we take the surface-delta interaction (SDI). In a earlier paper [7] the formalism and some applications are presented. By comparison with low-seniority shell-model calculations (LSSM), we demonstrated the importance of including particle-number projection in the BCS approximation, and that the PBCS yields results very close to those obtained with LSSM.

For odd-mass isotones, previous calculations generally are restricted to seniority-one degrees of freedom. Exclusively in Refs. [1–3], three-quasiparticle excitations are incorporated but without particle-number conservation. In addition, in recent years several experimental studies of odd-mass $N=82$ isotones have been carried out, which provide much new data on spectra, electromagnetic properties, and high-spin states [8–12].

Theoretical studies were performed, in some cases, by restricted shell-model (SM) calculations [13–16]. The ^{137}Cs isotone is analyzed by Baldridge [13] in the small proton space $(g_{7/2},d_{5/2})^5$, and only for states with spin and parity $I^{\pi}=\frac{1}{2}^+$, the single-particle orbitals $h_{11/2}$, $d_{3/2}$, and $s_{1/2}$ have been included. In Ref. [14] the ^{143}Pm nucleus is described by Prade *et al.* within a space where proton configurations of the types $(g_{7/2},d_{5/2})^{Z-50}$ and $(g_{7/2},d_{5/2})^{Z-51}(d_{3/2},s_{1/2})^1$ have been taken into account. The structure of positive-parity high-spin $\leq \frac{11}{2}$ states in ^{141}Pr were investigated by Prade *et al.* [15] within the same space of Ref. [14], and for negative-parity states in ^{141}Pr and ^{143}Pm, the configurations $(g_{7/2},d_{5/2})^{Z-51}(h_{11/2})^1$ have been considered. Assuming ^{146}Gd to be a doubly closed-shell nucleus, Kaczarowski *et al.* [16] have interpreted the negative-parity high-spin levels of the ^{145}Eu nucleus as members of $(d_{5/2})^{-2}(h_{11/2})^1$ and $(d_{5/2},g_{7/2})^{-2}(h_{11/2})^1$ multiplets.

In this paper a systematic examination of the properties of low-lying states of odd-mass $N=82$ isotones are presented. Our study encompasses the isotones ^{137}Cs, ^{139}La, ^{141}Pr, ^{143}Pm, and ^{145}Eu. We focus our attention on the positive-parity states. In future work, the study of the positive- and negative-parity high-spin states shall be developed.

II. PARAMETERS

We describe the states of $N=82$ isotones, with $55 \leq Z \leq 63$, assuming $^{132}_{50}\mathrm{Sn}_{82}$ as a inert core. The low-lying levels are assumed to come from 5 to 13 protons distributed over the single-particle orbitals $1g_{7/2}$, $2d_{5/2}$, $3s_{1/2}$, $2d_{3/2}$, and $1h_{11/2}$. A surface-delta interaction is used as the residual nucleon-nucleon interaction

$$V_{\mathrm{SDI}}=-4\pi G\delta(r_i-R)\delta(r_j-R)\delta(\Omega_{ij}) .$$

Our starting point for the choice of parameters was based on the values used in Ref. [5], for $55 \leq Z \leq 61$, and in Ref. [17], for $Z=63$. The final values were determined by requiring a good overall fit of the energies of one-quasiparticle (1qp) states, and a reasonable density of low-energy levels. Parameters used in the present calculations are summarized in Table I. It should be noted that the single-particle energies decrease with the mass number. The same behavior was observed experimentally

TABLE I. Parameters used in the present calculations.

	^{137}Cs	^{139}La	^{141}Pr	^{143}Pm	^{145}Eu (A)	^{145}Eu (B)
$\varepsilon_{g_{7/2}}$ (MeV)	0.0	0.0	0.0	0.0	0.0	0.0
$\varepsilon_{d_{5/2}}$ (MeV)	0.77	0.77	0.77	0.40	0.40	0.35
$\varepsilon_{d_{3/2}}$ (MeV)	2.60	2.60	2.50	2.60	2.60	2.20
$\varepsilon_{s_{1/2}}$ (MeV)	2.62	2.50	2.50	2.30	2.30	1.90
$\varepsilon_{h_{11/2}}$ (MeV)	2.30	2.15	2.15	2.05	2.05	1.85
G (MeV)	0.17	0.17	0.17	0.165	0.165	0.13

TABLE II. Calculated wave functions of some low-lying (I^π) states in $N=82$ isotones. For each nucleus, the 1qp and 3qp basis states are denoted by $|j\rangle$ and $|(j_a j_b)J_{ab}, j_c\rangle$, respectively. Only amplitudes larger than 4% are listed. For the ^{145}Eu the plotted values were obtained with the set of parameter B.

I_i^π	j_a	j_b	J_{ab}	j_c	^{137}Cs	^{139}La	^{141}Pr	^{143}Pm	^{145}Eu
$\frac{7}{2}^+_1$				$\frac{7}{2}$	0.993	0.989	0.990	0.992	0.989
$\frac{5}{2}^+_1$				$\frac{5}{2}$	0.991	0.991	0.991	0.994	0.990
$\frac{11}{2}^-_1$				$\frac{11}{2}$	0.982	0.981	0.981	0.976	0.945
$\frac{3}{2}^+_1$				$\frac{3}{2}$		0.346	0.703		0.945
	$\frac{7}{2}$	$\frac{7}{2}$	2	$\frac{5}{2}$		0.564		−0.233	
	$\frac{5}{2}$	$\frac{5}{2}$	2	$\frac{7}{2}$		0.471	0.533		
	$\frac{7}{2}$	$\frac{7}{2}$	4	$\frac{7}{2}$	0.966				
	$\frac{7}{2}$	$\frac{7}{2}$	4	$\frac{5}{2}$		0.416			
	$\frac{5}{2}$	$\frac{5}{2}$	4	$\frac{5}{2}$				0.925	
$\frac{1}{2}^+_1$				$\frac{1}{2}$		0.324	0.813	0.971	0.961
	$\frac{7}{2}$	$\frac{7}{2}$	2	$\frac{5}{2}$	0.922	−0.854	−0.333		
	$\frac{5}{2}$	$\frac{5}{2}$	4	$\frac{7}{2}$	−0.254	0.337	0.402		
$\frac{9}{2}^+_1$	$\frac{7}{2}$	$\frac{7}{2}$	2	$\frac{5}{2}$		0.924			
	$\frac{5}{2}$	$\frac{5}{2}$	2	$\frac{7}{2}$			0.933		
	$\frac{7}{2}$	$\frac{7}{2}$	4	$\frac{7}{2}$	0.958				
	$\frac{7}{2}$	$\frac{7}{2}$	4	$\frac{5}{2}$	0.209	0.311			
	$\frac{5}{2}$	$\frac{5}{2}$	4	$\frac{7}{2}$				−0.253	
	$\frac{5}{2}$	$\frac{5}{2}$	4	$\frac{5}{2}$				0.930	0.212
	$\frac{5}{2}$	$\frac{5}{2}$	4	$\frac{1}{2}$					0.662
	$\frac{5}{2}$	$\frac{5}{2}$	4	$\frac{3}{2}$					−0.556
	$\frac{7}{2}$	$\frac{5}{2}$	4	$\frac{1}{2}$					−0.227
	$\frac{7}{2}$	$\frac{5}{2}$	5	$\frac{3}{2}$					0.221
	$\frac{7}{2}$	$\frac{5}{2}$	6	$\frac{3}{2}$					0.258
$\frac{15}{2}^+_1$	$\frac{7}{2}$	$\frac{7}{2}$	4	$\frac{7}{2}$	0.924				
	$\frac{7}{2}$	$\frac{7}{2}$	6	$\frac{5}{2}$	−0.376	0.922			
	$\frac{7}{2}$	$\frac{7}{2}$	4	$\frac{7}{2}$		−0.352			
	$\frac{5}{2}$	$\frac{5}{2}$	4	$\frac{7}{2}$			0.993	0.993	
$\frac{13}{2}^+_1$	$\frac{7}{2}$	$\frac{7}{2}$	4	$\frac{5}{2}$	0.909	0.921			
	$\frac{7}{2}$	$\frac{7}{2}$	6	$\frac{5}{2}$	0.402				
	$\frac{5}{2}$	$\frac{5}{2}$	4	$\frac{7}{2}$			0.976	0.975	
	$\frac{7}{2}$	$\frac{5}{2}$	6	$\frac{1}{2}$					0.952
	$\frac{7}{2}$	$\frac{7}{2}$	6	$\frac{1}{2}$					0.240

[18]. The density of levels above 1 MeV and the energy of the three-quasiparticle (3qp) states are sensitive to the relative single-particle energies $\varepsilon d_{5/2}$-$\varepsilon d_{7/2}$ and $\varepsilon h_{11/2}$-$\varepsilon g_{7/2}$, and to small variations in the intensive strength G. Our values for the parameter G agrees with that obtained by Chasman [19], using the method of correlated quasiparticles, in which the correlations arising from particle number conservation, usually neglected in BCS approximation, are included. The blocking effect is fully taken into account.

The electromagnetic properties were evaluated with the usual values [1,3,14,15] for the effective electric charge and the effective gyromagnetic ratios, namely, $e_p^{\text{eff}}=e$, and $2e$, for electric transitions, and $g_l=1$, $g_s^{\text{eff}}=2.234$, 2.91, 3.91, 4.464, and 5.58 for the magnetic ones.

TABLE II. (*Continued*).

I_i^π	j_a	j_b	J_{ab}	j_c	^{137}Cs	^{139}La	^{141}Pr	^{143}Pm	^{145}Eu
$\frac{11}{2}\,1^+$	$\frac{5}{2}$	$\frac{5}{2}$	2	$\frac{7}{2}$			0.933	0.911	
	$\frac{7}{2}$	$\frac{7}{2}$	4	$\frac{7}{2}$	0.943	0.272			
	$\frac{7}{2}$	$\frac{7}{2}$	4	$\frac{5}{2}$	0.209	0.952			
	$\frac{5}{2}$	$\frac{5}{2}$	4	$\frac{7}{2}$			0.296	0.351	
	$\frac{7}{2}$	$\frac{5}{2}$	6	$\frac{1}{2}$					0.584
	$\frac{7}{2}$	$\frac{5}{2}$	5	$\frac{1}{2}$					−0.445
$\frac{7}{2}\,2^+$	$\frac{7}{2}$	$\frac{7}{2}$	0	$\frac{7}{2}$		−0.626			
	$\frac{5}{2}$	$\frac{5}{2}$	4	$\frac{1}{2}$					0.922
	$\frac{7}{2}$	$\frac{7}{2}$	2	$\frac{5}{2}$	0.964	0.712			
	$\frac{5}{2}$	$\frac{5}{2}$	2	$\frac{7}{2}$			0.866	0.895	
	$\frac{5}{2}$	$\frac{5}{2}$	4	$\frac{7}{2}$			−0.348	−0.249	
	$\frac{7}{2}$	$\frac{5}{2}$	5	$\frac{3}{2}$					0.241
$\frac{5}{2}\,2^+$	$\frac{7}{2}$	$\frac{7}{2}$	0	$\frac{5}{2}$			0.789	−0.579	0.275
	$\frac{5}{2}$	$\frac{5}{2}$	0	$\frac{5}{2}$			−0.309	0.345	0.549
	$\frac{7}{2}$	$\frac{7}{2}$	2	$\frac{5}{2}$		−0.687	0.225	−0.317	
	$\frac{5}{2}$	$\frac{5}{2}$	2	$\frac{7}{2}$		0.410	−0.341	0.521	
	$\frac{7}{2}$	$\frac{7}{2}$	4	$\frac{7}{2}$	0.956	0.425			
	$\frac{7}{2}$	$\frac{7}{2}$	4	$\frac{5}{2}$		0.283			
	$\frac{5}{2}$	$\frac{5}{2}$	4	$\frac{7}{2}$				0.207	
	$\frac{5}{2}$	$\frac{5}{2}$	2	$\frac{3}{2}$					0.688
	$\frac{7}{2}$	$\frac{5}{2}$	2	$\frac{1}{2}$					0.208
$\frac{1}{2}\,2^+$				$\frac{1}{2}$	0.924	0.914	0.543		
	$\frac{7}{2}$	$\frac{7}{2}$	2	$\frac{5}{2}$	0.240	0.316	0.421	−0.539	
	$\frac{5}{2}$	$\frac{5}{2}$	4	$\frac{7}{2}$	−0.250		−0.669	0.764	
	$\frac{7}{2}$	$\frac{5}{2}$	1	$\frac{3}{2}$				0.203	0.432
	$\frac{5}{2}$	$\frac{5}{2}$	2	$\frac{3}{2}$					0.655
	$\frac{7}{2}$	$\frac{5}{2}$	2	$\frac{3}{2}$					0.398
	$\frac{7}{2}$	$\frac{7}{2}$	0	$\frac{1}{2}$					−0.344
$\frac{3}{2}\,2^+$				$\frac{3}{2}$				0.821	
	$\frac{7}{2}$	$\frac{7}{2}$	2	$\frac{5}{2}$	0.754	−0.638	−0.329		
	$\frac{7}{2}$	$\frac{7}{2}$	4	$\frac{5}{2}$	0.443	0.371			
	$\frac{5}{2}$	$\frac{5}{2}$	2	$\frac{7}{2}$	0.277	0.308		0.409	
	$\frac{7}{2}$	$\frac{7}{2}$	4	$\frac{7}{2}$		−0.336			
	$\frac{5}{2}$	$\frac{5}{2}$	4	$\frac{5}{2}$		0.332	0.817		0.221
	$\frac{5}{2}$	$\frac{5}{2}$	4	$\frac{7}{2}$			−0.239		
	$\frac{5}{2}$	$\frac{5}{2}$	2	$\frac{1}{2}$					0.900
	$\frac{7}{2}$	$\frac{5}{2}$	3	$\frac{3}{2}$					0.207

III. RESULTS AND DISCUSSION

A. Energy spectra

The experimental and calculated level schemes of the energy spectra for ^{137}Cs, ^{139}La, ^{141}Pr, ^{143}Pm, and ^{145}Eu are compared in Figs. 1–5. We have calculated all possible low-lying positive-parity states with excitation energy below 2.0 MeV, for $Z \leq 61$, and up to 2.20 MeV, for $Z = 65$. In order to complete the results for 1qp, states the negative-parity $\frac{11}{2}_1^-$ states are included.

We connect by dotted line 1qp states and those with mixed 1qp and 3qp components with the probably correspondent experimental ones, based on the spectro-

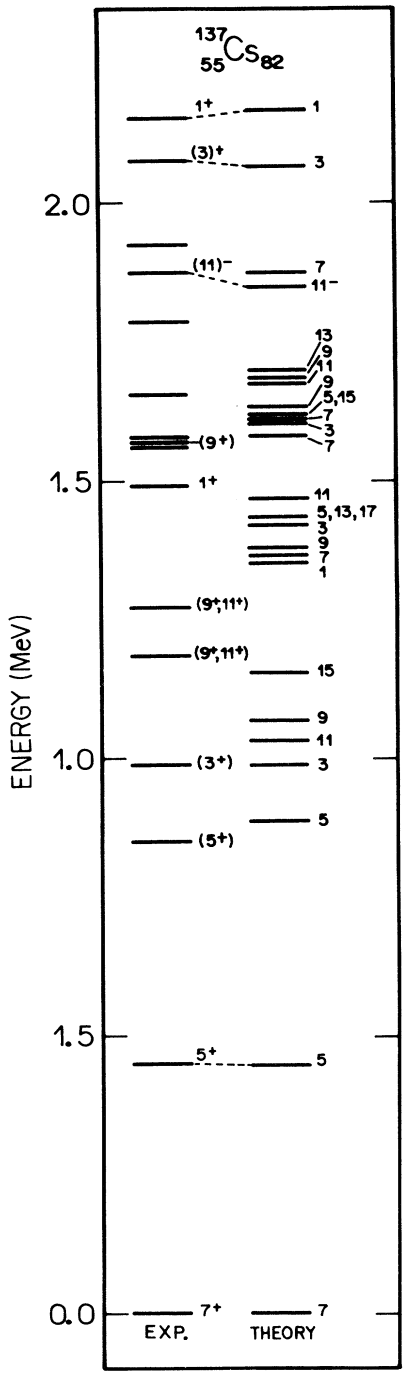

FIG. 1. Calculated and experimental [8] spectrum of ^{137}Cs. Dotted lines connect one-quasiparticle states. The spins are in $2J$ form. All theoretical states have positive parity unless noted otherwise.

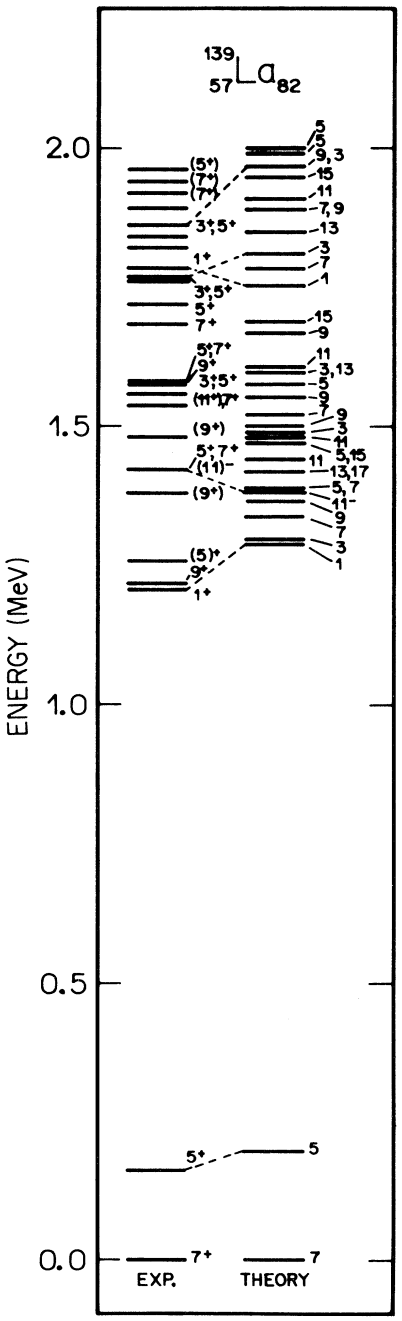

FIG. 2. Calculated and experimental [9] spectrum of ^{139}La. See Fig. 1 caption.

scopic factors calculated by Wildenthal *et al.* [20].

Due to the high density of levels above 1-MeV excitation energy, the one-to-one identification of the experimental and calculated 3qp states turns out to be, in general, quite difficult and uncertain. Therefore, in the following discussion of the 3qp states, only a tentative identification with experimental levels will be presented.

In Table II, wave functions calculated for a few low-lying states are listed. There is good agreement, in general, between experimental and theoretical energy spectra. The differences in energy for dominant 1qp states is ≤ 50 keV, and for states with (1qp+3qp) mixing character is ≤ 100 keV. All other experimentally known levels below 2 MeV can be assigned as being 3qp states and differ less than 200 keV in energy. Below, we present a short discussion for each nucleus separately.

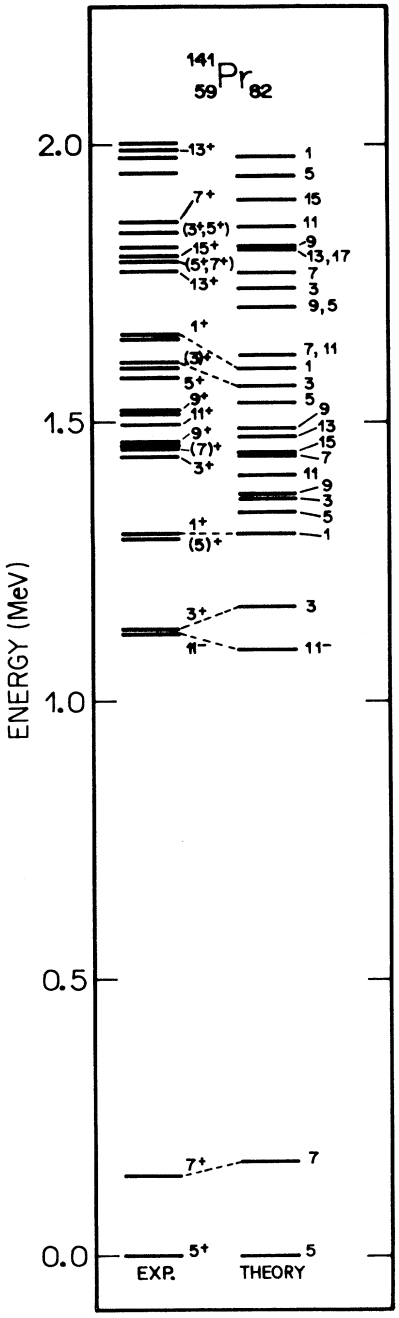

FIG. 3. Calculated and experimental [10] spectrum of ^{141}Pr. See Fig. 1 caption.

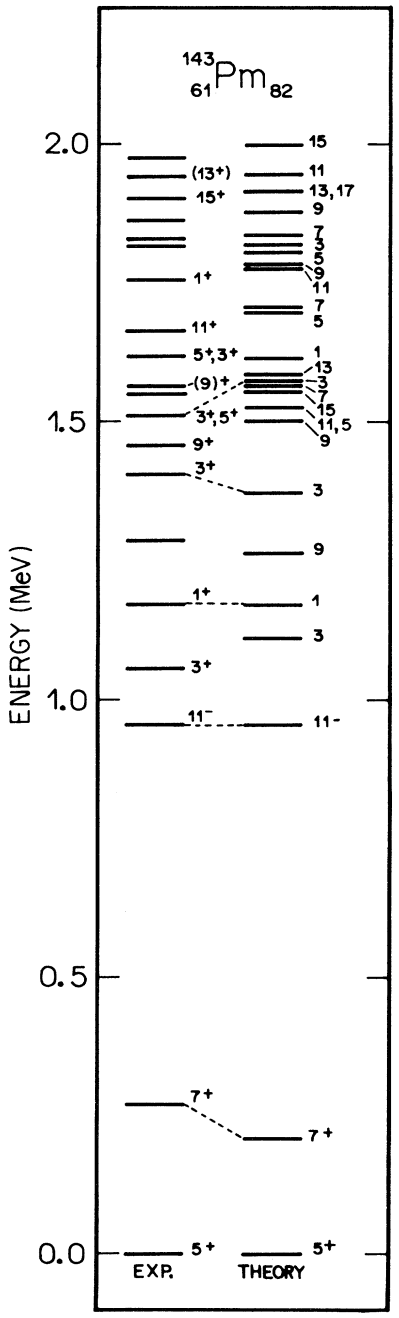

FIG. 4. Calculated and experimental [11] spectrum of ^{143}Pm. See Fig. 1 caption.

(a) ^{137}Cs. Our theoretical spectrum is similar to earlier calculations [2,3,20]. All theoretical results indicate the sequence of low-lying levels to be $J^\pi = \frac{7}{2}^+$, $\frac{5}{2}^+$, $\frac{5}{2}^+$, $\frac{3}{2}^+$, $\frac{11}{2}^+$, and $\frac{9}{2}^+$. It reinforces the $\frac{5}{2}^+$ and $\frac{3}{2}^+$ spin assignments for the experimental levels at 0.849 and 0.981 MeV, respectively, and suggests $\frac{11}{2}^+$ and $\frac{9}{2}^+$ spin and parity assignments for the levels measured at 1.184 and 1.273 MeV, respectively. In addition, we predict a $\frac{15}{2}^+$ state at about 1 MeV, and two states with $I^\pi = \frac{17}{2}^+$ and $\frac{15}{2}^+$ at about 1.5 MeV. The 3qp $\frac{1}{2}^+_1$ state may correspond to the $\frac{1}{2}^+$ experimental level at 1.49 MeV.

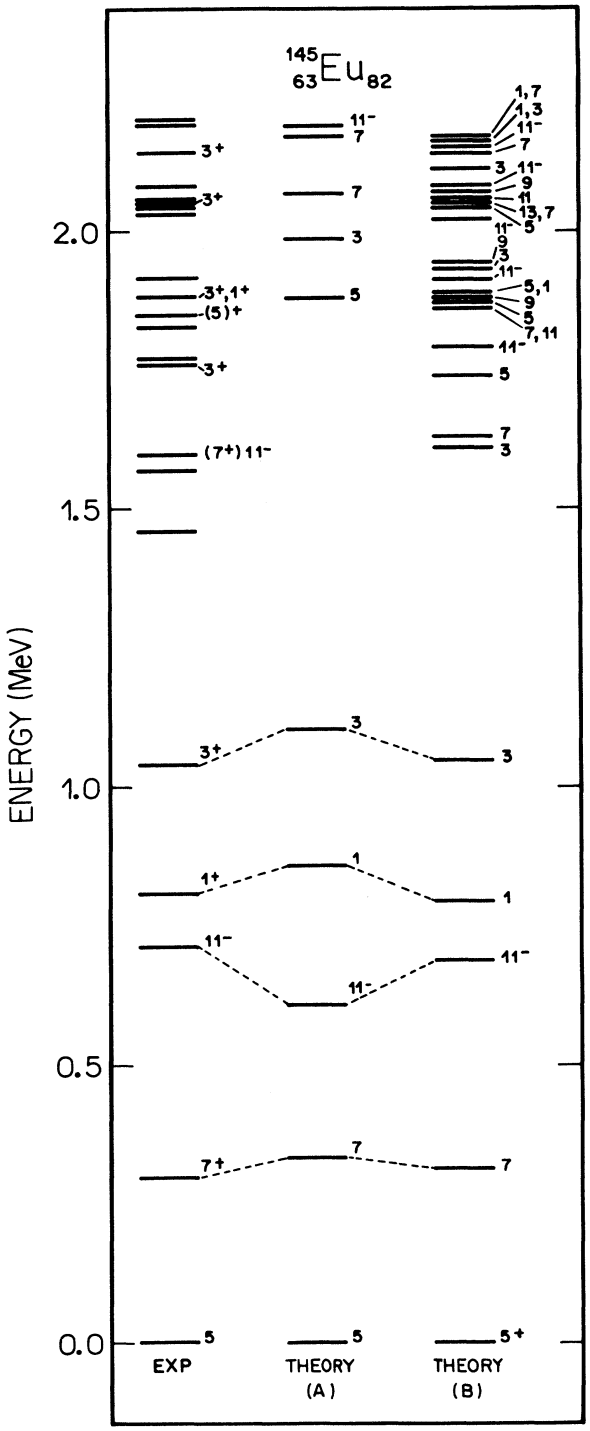

FIG. 5. Calculated and experimental [12] spectrum of ^{145}Eu. See Fig. 1 caption.

(b) ^{139}La. The experimental density of levels in the region 1–2 MeV is well reproduced by our calculation, in contrast with that carried out in Ref. [1], in which the same SDI force was used, and in agreement with those calculated in Refs. [2] and [3], using Elliott and Gaussian interactions, respectively. Similar to the spectra obtained in Ref. [2], the number of levels for $J^\pi \leq \frac{9}{2}^+$, up to 2 MeV, is the same obtained experimentally. No state with $J^\pi > \frac{9}{2}^+$ was calculated in Ref. [2]. In Ref. [3] the number of $\frac{5}{2}^+$ and $\frac{7}{2}^+$ states is smaller than the experimental one. For high-spin states with $J^\pi \geq \frac{11}{2}^+$, our results foretell one more state by spin than those obtained in Ref. [3], and an additional $\frac{17}{2}^+$ state at very low energy (about 1.5 MeV).

(c) ^{141}Pr. The theoretical spectrum reproduces the experimental sequence for the first four levels, i.e., $\frac{5}{2}^+$, $\frac{7}{2}^+$, $\frac{11}{2}^-$, and $\frac{3}{2}^+$. The density of levels in the region 1–2 MeV is in good agreement with experiment. Similar results have been obtained in Ref. [2], where only states with $J^\pi \leq \frac{9}{2}^+$ were considered. The two low-lying levels measured at 1.29 and 1.45 MeV probably have $\frac{5}{2}^+$ and $\frac{7}{2}^+$ spin assignments, respectively, which may correspond to the theoretical $\frac{5}{2}^+_2$ and $\frac{7}{2}^+_2$ states established at 1.34 and 1.44 MeV. The 3qp states $\frac{3}{2}^+_2$, $\frac{9}{2}^+_1$, $\frac{9}{2}^+_2$, $\frac{5}{2}^+_3$, and $\frac{1}{2}^+_2$, may be related to the experimental levels at 1.44, 1.46, 1.52, 1.58, and 1.66 MeV, respectively. Just as in ^{137}Cs and ^{139}La, $J^\pi = \frac{11}{2}^+$, $\frac{13}{2}^+$, $\frac{15}{2}^+$, and $\frac{17}{2}^+$ states are calculated. The agreement between our calculated spectrum and that obtained with a shell model [15] is remarkable. Both present the same number of states by spin. Two states with $J^\pi = \frac{13}{2}^+$ and $\frac{15}{2}^+$ at about 1.5 MeV, and one $\frac{17}{2}^+$ state at 1.8 MeV are predicted. The 3qp $\frac{11}{2}^+_1$, $\frac{13}{2}^+_2$, and $\frac{15}{2}^+_2$ states may correspond to the levels measured at 1.49, 1.77, and 1.80 MeV excitation energy, respectively.

(d) ^{143}Pm. The experimental sequence of low-lying levels $\frac{5}{2}^+$, $\frac{7}{2}^+$, $\frac{11}{2}^-$, $\frac{3}{2}^+$, and $\frac{1}{2}^+$ is reproduced. For the density of level in the region of 1.5–2.0 MeV, we have analogous results, as in the ^{141}Pr case, to the comparison with experimental data and the spectra obtained in Refs. [1–3]. J^π states $\frac{11}{2}^+$, $\frac{13}{2}^+$, $\frac{15}{2}^+$, and $\frac{17}{2}^+$ are also calculated. We propose a spin and parity assignment $\frac{13}{2}^+$ to the level measured at 1.94 MeV, which can be related to the $\frac{13}{2}^+_2$ state. The 3qp $\frac{5}{2}^+_2$, $\frac{3}{2}^+_3$, $\frac{1}{2}^+_2$, and $\frac{15}{2}^+_2$ states probably correspond to experimental levels at 1.51, 1.75, and 1.90 MeV, respectively, and the measured level $\frac{11}{2}^+$ at 1.66 MeV corresponds to the $\frac{11}{2}^+_1$ or $\frac{11}{2}^+_2$ state. Our calculation foresees two states with $J^\pi = \frac{15}{2}^+$ and $\frac{13}{2}^+$ and one $\frac{17}{2}^+$ state, at about 1.5 and 2.0 MeV, respectively. The resemblance with a standard shell-model calculation [14] is again remarkable.

(e) ^{145}Eu. In order to illustrate the sensitivity of 3qp

TABLE III. Comparison between experiment and theory. The magnetic dipole (μ) and electric quadrupole (Q) are in units e b and μ_N, respectively. The transition probabilities $B(M1)$ and $B(E2)$ are in units of $10^{-3}\mu_N$ and $10^{-3}\ e^2\,\mathrm{b}^2$, respectively. The subscript 1 refers to $g_s^{\mathrm{eff}}=2.234$ or $e^{\mathrm{eff}}=e$, 2 refers to $g_s^{\mathrm{eff}}=2.91$ or $e^{\mathrm{eff}}=2e$, 3 refers to $g_s=3.91$, 4 refers to $g_s=4.464$, and 5 refers to $g_s=5.58$. For the ^{145}Eu nucleus, the plotted values were obtained with parametrization (B). The asterisk indicates WU units.

Nucleus	Quantity		Experiment		Theory				
					1	2	3	4	5
^{137}Cs		$\mu_{7/2_1^+}$	+2.841 3	4[a]	+3.02	+2.76	+2.37	+2.16	+1.72
		$Q_{7/2_1^+}$	+0.051	1[a]	+0.024	+0.048			
^{139}La		$\mu_{7/2_1^+}$	+2.761 465 8	22[b]	+3.02	+2.76	+2.37	+2.15	+1.72
		$Q_{7/2_1^+}$	+0.22	3[b]	+0.10	+0.20			
	$B(M1)$	$\frac{5}{2}_1^+ \to \frac{7}{2}_1^+$	0.002 57*	4[b]	$<10^{-3}$	$<10^{-3}$	$<10^{-3}$	$<10^{-3}$	$<10^{-3}$
		$\frac{9}{2}_1^+ \to \frac{7}{2}_1^+$	0.000 77*	17[b]	0.000 18	0.000 44	0.001 03	0.001 46	0.002 54
		$\frac{7}{2}_3^+ \to \frac{7}{2}_1^+$	0.070*	16[b]	$<10^{-3}$	$<10^{-3}$	$<10^{-3}$	$<10^{-3}$	$<10^{-2}$
		$\frac{7}{2}_3^+ \to \frac{5}{2}_1^+$	0.11*	16[b]	$<10^{-3}$	$<10^{-3}$	$<10^{-3}$	$<10^{-3}$	$<10^{-3}$
	$B(E2)$	$\frac{5}{2}_1^+ \to \frac{7}{2}_1^+$	≤ 8[b]		8	32			
			<2[b]*		0.02	0.07			
		$\frac{9}{2}_1^+ \to \frac{7}{2}_1^+$	40	6[b]	6	24			
			7.5	1.1[b]*	0.01	0.06			
		$\frac{9}{2}_1^+ \to \frac{5}{2}_1^+$	1.79	24[b]*	1.41	5.62			
		$\frac{5}{2}_2^+ \to \frac{7}{2}_1^+$	12	4[b]	246	986			
			3.7	1.3[b]*	0.6	2.3			
		$\frac{5}{2}_3^+ \to \frac{7}{2}_1^+$	15.0	1.5[b]	867	3470			
			4.7	5[b]*	2.0	8.1			
		$\frac{7}{2}_2^+ \to \frac{7}{2}_1^+$	15.0	1.5[b]	131	523			
			3.5	4[b]*	0.3	1.2			
		$\frac{7}{2}_3^+ \to \frac{7}{2}_1^+$	60	6[b]	6	24			
			14.0	1.4[b]*	0.01	0.06			
		$\frac{7}{2}_3^+ \to \frac{5}{2}_1^+$	23	10[b]*	0.6	2.4			
		$\frac{7}{2}_4^+ \to \frac{7}{2}_1^+$	59	5[b]	8	30			
			13.8	1.2[b]*	0.01	0.08			
		$\frac{3}{2}_4^+ \to \frac{7}{2}_1^+$	47	7[b]	109	436			
			22	4[b]*	0.3	1.0			
^{141}Pr		$\mu_{5/2_1^+}$	+4.275 4	5[c]	+3.12	+3.45	+3.96	+4.23	+4.79
		$\mu_{7/2_1^+}$	+2.8	2[c]	+3.01	+2.74	+2.35	+2.13	+1.69
		$\mu_{11/2_1^-}$	+7.2	4[c]	+6.1	+6.5	+7.0	+7.2	+7.8
		$Q_{5/2_1^+}$	−0.058 9	42[c]	−0.08	−0.17			
	$B(M1)$	$\frac{7}{2}_1^+ \to \frac{5}{2}_1^+$	4.84	30[d]	$<10^{-3}$	$<10^{-3}$	$<10^{-3}$	$<10^{-3}$	$<10^{-3}$
		$\frac{15}{2}_2^+ \to \frac{13}{2}_2^+$	171	25[d]	15	32	74	119	207
	$B(E2)$	$\frac{7}{2}_1^+ \to \frac{5}{2}_1^+$	2.5	4[c]	0.6	2.4			
		$\frac{3}{2}_1^+ \to \frac{5}{2}_1^+$	12.6	1.3[c]	5.9	23.7			
		$\frac{5}{2}_2^+ \to \frac{5}{2}_1^+$	23	2[c]	198	795			
		$\frac{3}{2}_3^+ \to \frac{5}{2}_1^+$	10.5	1.1[c]	7.5	30.0			
		$\frac{15}{2}_2^+ \to \frac{11}{2}_2^+$	4.0	4[d]	9.4	4.8			

TABLE III. (*Continued*).

Nucleus	Quantity		Experiment		Theory				
					1	2	3	4	5
^{143}Pm		$\mu_{5/2_1^+}$	+3.9	6[e]	+3.2	+3.5	+4.0	+4.3	+4.94
		$\mu_{11/2_1^-}$	+6.27	50[e]	+6.13	+6.48	+6.99	+7.28	+7.85
		$\mu_{15/2_2^+}$	+7.50	43[e]	+7.08	+6.85	+6.51	+6.32	+5.94
	$B(M1)$	$\frac{7}{2}_1^+ \rightarrow \frac{5}{2}_1^+$	1.64	12[f]	0.12	0.30	0.69	0.98	1.71
			0.000 94	7[e]	0.000 07	0.000 17	0.000 39	0.000 55	0.000 95
	$B(E2)$	$\frac{7}{2}_1^+ \rightarrow \frac{5}{2}_1^+$	<0.17[e]*		0.02	0.08			
		$\frac{15}{2}_2^+ \rightarrow \frac{11}{2}_1^+$	6.4	4[f]	4.3	17.2			
^{145}Eu		$\mu_{5/2_1^+}$	+1.1	3[g]	+3.20	+3.58	+4.15	+4.46	+5.09
		$\mu_{11/2_1^-}$	+7.458	44[g]	+6.50	+6.50	+7.03	+7.32	+7.90

[a]Reference [8].
[b]Reference [9].
[c]Reference [10].
[d]Reference [15].
[e]Reference [11].
[f]Reference [14].
[g]Reference [12].

states with respect to the parameter G, we present the theoretical spectra for $G=0.165$ MeV, theory (A), and for $G=0.13$, theory (B). There is very good agreement between the theory (B) calculated spectrum and the experimental one. The same prediction of weak proton pairing interaction strength in this mass region, near $Z=64$, was anticipated by Chasman [19]. In our calculated spectra [theory (B)], the experimental density of levels about 1.5 MeV is well reproduced. Earlier calculations had quite different results. The spectrum obtained in Ref. [3] is similar to that calculated with the parametrization (A). In Ref. [2], the experimental energy gap at about 500 keV above the single-particle levels does not exist, and the 3qp states are lowered too much. The theoretical spectra performed with parametrization (B) [theory (B)], suggests spin and parity assignments $\frac{7}{2}^+$ to the level measured at 1.60 MeV, and predict 3qp spin $\frac{11}{2}_2^-$ and $\frac{1}{2}_1^+$ states at 1.79 and 1.89 MeV, which may correspond to the levels seen at 1.60 and 1.88 MeV, respectively. Only above 2 MeV excitation energy are states with $J^\pi \geq \frac{13}{2}^+$ prognosticated.

TABLE IV. Calculated electric quadrupole and magnetic dipole moments, in units of e b and μ_N, respectively. Q_1 refers to $e_p^{\text{eff}}=2e$, μ_1, μ_2 refer to $g_s^{\text{eff}}=2.91$ and $g_s^{\text{eff}}=4.464$, respectively.

Level	^{137}Cs			^{141}Pr			^{145}Eu		
	Q_1	μ_1	μ_2	Q_1	μ_1	μ_2	Q_1	μ_1	μ_2
$\frac{7}{2}_1^+$	0.05	2.76	2.16	0.27	2.74	2.13	0.34	2.69	2.03
$\frac{5}{2}_1^+$	−0.25	3.44	4.20	−0.17	3.46	4.23	0.28	3.58	4.46
$\frac{11}{2}_1^-$	−0.44	6.45	7.21	−0.43	6.45	7.23	−0.42	6.50	7.32
$\frac{3}{2}_1^+$	−0.02	1.18	0.92	−0.11	0.82	0.27	−0.22	0.91	0.43
$\frac{1}{2}_1^+$		1.11	1.60		1.39	2.12		1.53	2.37
$\frac{7}{2}_2^+$	−0.12	3.89	4.20	0.07	3.18	2.92	0.20	4.23	4.82
$\frac{5}{2}_2^+$	0.10	1.99	1.57	0.04	3.26	3.87	−0.02	3.84	4.92
$\frac{3}{2}_2^+$	−0.03	1.47	1.45	0.07	2.03	2.46	−0.09	1.65	1.77
$\frac{1}{2}_2^+$		1.45	2.24		1.49	2.30		1.26	1.87
$\frac{9}{2}_1^+$	0.006	3.62	2.90	0.11	4.36	4.24	0.02	6.30	7.76
$\frac{11}{2}_1^+$	−0.03	4.36	3.44	0.17	5.62	5.72	0.23	5.81	6.06
$\frac{13}{2}_1^+$	−0.22	6.44	6.40	0.04	7.19	7.74	0.41	7.56	8.42
$\frac{15}{2}_1^+$	0.06	6.06	4.88	0.11	8.33	9.00	0.32	7.22	7.00
$\frac{17}{2}_1^+$	−0.30	8.18	7.92	0.22	8.18	7.92	−0.21	10.11	11.42

B. Electromagnetic properties

The available experimental data [8–12,14,15] on the magnetic dipole (μ) and electric quadrupole (Q) moments and the $B(M1)$ and $B(E2)$ transition probabilities are presented and compared with the calculated values for the odd $N=82$ isotones in Table III. With the exception of the $\mu_{5/2_1^+}$ in ^{145}Eu nucleus, the experimental moments are fairly well reproduced by theoretical calculation. It should be noted, however, that the measured magnetic moments for the ground state in the neighboring ^{141}Pr and ^{143}Pm isotones have magnitudes close to the single-particle estimative, about $4\mu_N$. Keeping in mind the uncertainties in the measured values, there is good agreement between theoretical and experimental $B(E2)$ values, and $B(M1)$ values for transition $\frac{5}{2}1^+ \rightarrow \frac{7}{2}1^+$ in ^{139}La and ^{143}Pm nuclei, and for the transition $\frac{15}{2}2^+ \rightarrow \frac{13}{2}2^+$ in ^{141}Pr. The discrepancy in the other $M1$ transition seems to come from the fact that the role played by the tensor $M1$ operator $[Y_2 \times S]_1$, very important when the transition—due to l forbiddeness—is weak, is not considered in the present work.

In view of the excellent agreement verified for the electromagnetic moments, in Table IV, the magnetic dipole and electric quadrupole moments calculated for some low-lying states in ^{137}Cs, ^{141}Pr, and ^{145}Eu isotones are displayed. We thought it unnecessary to show the results for ^{139}La and ^{143}Pm as most of them fall in between the corresponding results for the neighboring nuclei. These theoretical foresights are presented in order to furnish a guide for future measurements.

IV. SUMMARY AND CONCLUSIONS

The properties of the odd $N=82$ isotones, in the mass region $137 \leq A \leq 145$, were performed within the framework of the projected 1qp+3qp calculations (PBCS) using an SDI force as the residual interaction. The different input parameters, proton single-particle energies, and interaction strength were obtained via an overall fit to 1qp state excitation energies and requiring a reasonable density of levels at low-energy spectra. All available data on the energy spectra, magnetic and electric moments, and $B(M1)$ and $B(E2)$ values were examined.

We can state that the present model describes the main features of the experimental level schemes and the electromagnetic properties of the low-lying states. Significant improvement is obtained with respect to earlier 1qp+3qp calculations [1–3] carried out without number-projected states.

ACKNOWLEDGMENTS

We would like to thank F. Krmpotić for fruitful discussions and W. A. Seale for critical reading of the manuscript. This work was supported in part by the FAPESP and CNPq.

[1] M. Waroquier and K. Heyde, Nucl. Phys. **A144**, 481 (1970).
[2] N. Freed and W. Miles, Phys. Lett. **32B**, 313 (1970).
[3] K. Heyde and M. Waroquier, Nucl. Phys. **A167**, 545 (1971).
[4] M. Waroquier and K. Heyde, Nucl. Phys. **A164**, 113 (1971).
[5] G. Wenes, K. Heyde, M. Waroquier, and P. Van Isacker, Phys. Rev. C **26**, 1692 (1982).
[6] F. Andreozzi, A. Covello, A. Gargano, and A. Porrino, Phys. Rev. C **41**, 250 (1989).
[7] L. Losano, H. Dias, F. Krmpotić, and B. H. Wildenthal, Phys. Rev. C **38**, 2902 (1988).
[8] L. K. Peker, Nucl. Data Sheets **38**, 87 (1983).
[9] T. Burrows, Nucl. Data Sheets **57**, 337 (1989).
[10] L. K. Peker, Nucl. Data Sheets **45**, 1 (1985).
[11] L. K. Peker, Nucl. Data Sheets **48**, 753 (1986).
[12] L. K. Peker, Nucl. Data Sheets **49**, 1 (1986).
[13] W. J. Baldridge, Phys. Rev. C **18**, 530 (1978).
[14] H. Prade, L. Käubler, U. Hagemann, H. U. Jäger, M. Kirchbach, L. Schneider, F. Stary, Z. Roller, and V. Paar, Nucl. Phys. **A333**, 33 (1980).
[15] H. Prade, W. Enghardt, H. U. Jäger, L. Käubler, H. J. Keller, and F. Stary, Nucl. Phys. **A370**, 47 (1981).
[16] R. Kaczarowski, E. G. Funk, and J. W. Mihelich, Phys. Rev. C **33**, 2711 (1981).
[17] C. Conci, V. Klemt, and J. Speth, Phys. Lett. **148B**, 405 (1984).
[18] Y. A. Akovali, K. S. Toth, A. L. Goodman, J. M. Nitschke, P. A. Wilmarth, D. M. Moltz, M. N. Rao, and D. C. Sousa, Phys. Rev. C **41**, 1126 (1990).
[19] R. R. Chasman, Phys. Rev. C **21**, 456 (1980).
[20] B. H. Wildenthal, E. Newman, and R. L. Auble, Phys. Rev. C **3**, 1199 (1971).